

The Efficient Oxygen Reduction Catalysts Based on the Non-Noble Metal and Conducting Polymers

Tingting Yang¹, Min Wang², Xiuping Ju³, Jinsheng Zhao^{1,*}, Chonggang Fu^{1,*}

¹ Department of Chemistry, Liaocheng University, Liaocheng, 252059, P.R. China.

² Liaocheng People's Hospital, Liaocheng, 252000, P.R. China.

³ Dongchang College, Liaocheng University, Liaocheng, 252059, P.R. China.

*E-mail: j.s.zhao@163.com (j.s.zhao); cgfu@lcu.edu.cn (c.g.Fu)

Received: 15 October 2017 / Accepted: 10 November 2017 / Published: 12 November 2017

This paper describes the synthesis and assessment of a non-noble-metal electrocatalyst for oxygen reduction reaction (ORR). The transition-metal-coordinating nitrogen-doped carbon catalyst (M-N/C) is prepared by supporting copper ion on carbon-coated poly(2,7-dimethyl-10,12-di(thiophen-2-yl)thieno[3',4':5,6]pyrazino[2,3-f][1,10]phenanthroline) (PDTPP) complex to offer Cu-PDTPP/C/GC. The materials including PDTPP, PDTPP/C, and Cu-PDTPP/C are characterized by CV (cyclic voltammetry), RDE (rotating disk electrode) to confirm their catalytic performances. Among the four materials, Cu-PDTPP/C shows the best catalytic performance with the direct reduction of oxygen to water directly by a four-electron (4e) transferred process. The morphologies and chemical compositions of PDTPP/C, Cu-PDTPP/C were characterized by scanning electron microscopy (SEM) and X-ray photoelectron spectroscopy (XPS) methods respectively. It is revealed by the results that the copper ions have been coordinated to the composite and the M-N/C catalysts are successfully synthesized. According to these tests, this study essentially illustrates that Cu-PDTPP/C is an effective catalyst that can be used for ORR in fuel cells, such as microbial fuel cells, which conducted in an aqueous neutral medium.

Keywords: Oxygen reduction reaction; M-N-C electrocatalyst; Polymerization

1. INTRODUCTION

With the drying up of traditional fossil fuels and increasingly serious global warming, the development and application of sustainable energy has been one of the major problems which may influence the advancement of human society [1-2]. Among numerous renewable resources, fuel cell is a kind of most promising renewable energy due to its simple structure, abundant raw materials and

excellent specific energy. And fuel cell as an efficient, response quickly, environmentally friendly novel electricity-generation device which has attracted attentions of many researchers in recent years [3-4]. At present, the research of fuel cell has made great progress [5-6], and the bottleneck is the slow cathodic oxygen reduction reaction which may greatly delayed the commercialization of fuel cell. Thus it is imminent to develop catalysts with good electrochemical performance for ORR [7-8].

As we all known, Pt is the best oxygen reducing catalyst with high electrochemical performances in terms of activity and stability. However, the expensive price and the shortage reserves of metal platinum hinder its use in fuel cells. So a lot of research has been made in metal alloy catalyst to cut back the costs and improve the catalysis, both in China and abroad. Stamenkovic et al has studied the relationship between surface electronic structure and catalytic activity in Pt_3M ($M=Fe, Co, Ni, Ti, V$), revealed that the catalytic activity can be tuned through the relationship between the adsorption of intermediates and the degree of surface coverage [9-12]. Similarly, transition metal oxides are used as electrochemical catalyst to replace Pt, which can modify the electronic structure and improve the stability in neutral aqueous solution. In addition, transition metal oxides also possess the advantages of low cost, easy preparation and species diversity which has become research focus in fuel cell field [13-15]. In recent years, in addition to metal alloy and metal oxides, conductive polymers had been widely employed as ORR catalysts because of its conjugated structure, high chemical stability as well as the complexation ability with metal ions. To be specific, many materials including N-doped macrocyclic polymers, carbon support metal-coordinating polymers are found to exhibit good electrochemical catalytic performance for ORR [16-18].

The catalysts prepared in this work were based on the synthesis of a novel and nitrogen-riched conductive polymer, which also have the complexation sites with metal ions. Through a facile electropolymerization method, the polymer film could be coated on the conductive surfaces, such as glassy carbon electrode (GC), modified GC etc. The monomer 2,7-dimethyl-10,12-di(thiophen-2-yl)thieno[3',4':5,6]pyrazino[2,3-f][1,10]phenanthroline (DTPP) was firstly prepared by the routine method, and then polymerized on the GC surface, which was designated to PDTPP/GC in the present work. PDTPP/C/GC was obtained when the polymer was coated on the carbon power modified GC electrode. Cu-PDTPP/GC referred to the materials obtained by the complexation of copper ions with the PDTPP/GC electrode. Similarly, Cu-PDTPP/C/GC was obtained by the complexation of copper ions with the C/GC electrode. The nitrogen atoms in polymers provided binding sites for metal ($M=Cu$) (Scheme 1), and carbon materials were used to improve the conductivity and stability of those catalysts.

The electrochemical performance of the obtained catalysts were conducted by cyclic voltammetry (CV), rotating disk electrode (RDE), while their structure and composition were performed by scanning electron microscopy (SEM) and X-ray photoelectron spectroscopy (XPS) methods. Among four catalysts, Cu-PDTPP/C/GC showed a much excellent performance than that of PDTPP/GC, PDTPP/C/GC and Cu-PDTPP/GC, indicating metal complexation and carbon carrier can improve the ORR activities of the catalysts. Cu-PDTPP/C/GC has been shown a promising, efficient, stable, and low-cost ORR catalyst which may be used in some of the fuel cells that require neutral media, such as microbial fuel cell.

2. EXPERIMENT

2.1 Materials

The monomer DTPP (2,7-dimethyl-10,12-di(thiophen-2-yl)thieno[3',4':5,6]pyrazino[2,3-f][1,10]phenanthroline) used as the monomer for the preparation of polymers was prepared by the method previously reported [19-20]. Other reagents including K_2CO_3 , $NaH_2PO_4 \cdot 2H_2O$, $Na_2HPO_4 \cdot 12H_2O$, $CuSO_4 \cdot 5H_2O$, $K_3[Fe(CN)_6]$, $K_4[Fe(CN)_6] \cdot 6H_2O$, KCl, acetonitrile (ACN), dichloromethane (DCM) and Tetrabutylammonium hexafluorophosphate ($TBAPF_6$) were obtained from Aladdin Chemical Reagent Company (Shanghai, China) with analytical grade and used as received without any further purification.

2.2. Electrode preparations

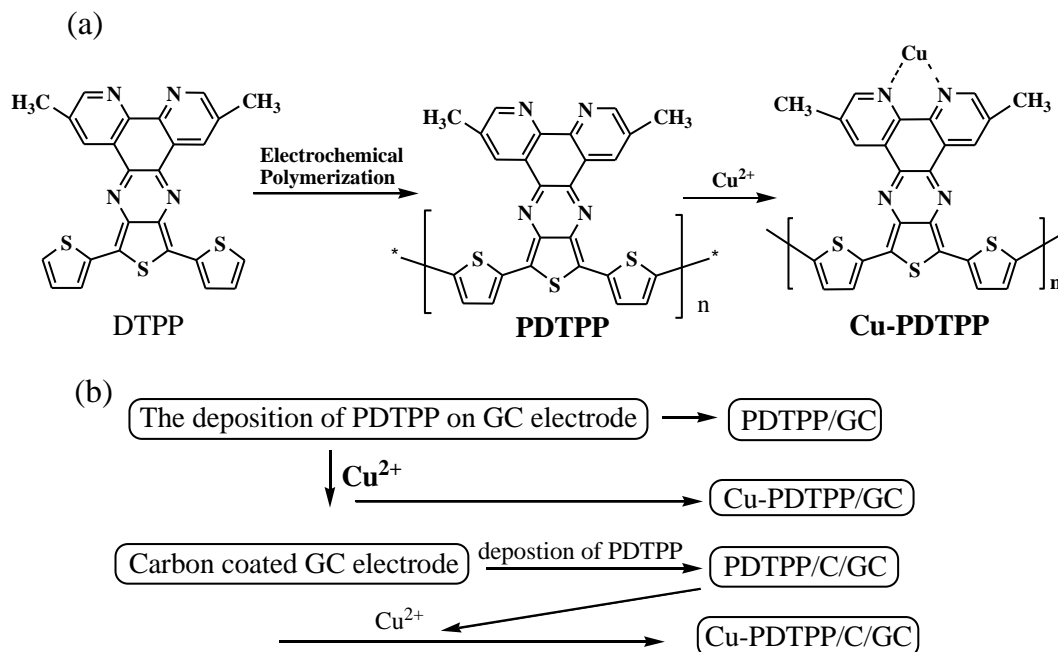
Alumina suspension (0.3 μm) was used to polish the glassy carbon electrode to a mirror surface, and the working electrode was washed with ultra-pure water and ethanol for several times to clean out excess powders. The mirror surface of GC could be used as the conductive surface for the coating of the PTPP polymer directly, or be coated with Vulcan carbon to obtain the GC/C electrode.

A carbon slurry could be obtained by the ultrasonic dispersion of a mixture solution containing 1.6 mg of the Vulcan XC-72 carbon, 177 μL of isopropanol, 570 μL of ultra-pure water, 3 μL of Nafion solution, and ultrasonic dispersion was conducted for at least 1 hour. The C/GC electrode could be obtained by dipping the above 8.5 μL of carbon dispersion drop on the glassy carbon electrode, dried in a clean console at room temperature for further studies.

The PDTPP/GC electrode was fabricated by using an electropolymerization process on the GC electrode ($\varphi=5mm$, $0.196 cm^2$, AFMSRCE pine). A solution used for polymerization was prepared by dissolving DTPP (4 mm) and $TBAPF_6$ (0.1 M) in DCM, the former is used as the monomer, and the latter as the supporting electrolyte. The three electrode system was used as the device for polymer forming, in which the GC electrode was used as the working electrode, a Pt coil was used as the counter electrode (area surface, $1cm^2$), and a silver wire was used as the pseudo reference electrode. Cyclic voltammetry (CV) was conducted in the above electrolyte for four cycles in the potential range from 0 to 1.3 V vs. Ag wire at scan rate of $100 mV s^{-1}$ on GC electrode. Subsequently, the obtained PDTPP/GC electrode was rinsed with ACN several times aimed to remove the residual monomer.

The Cu-PDTPP/GC electrode was prepared by soaking the PDTPP/GC electrode in 5 mM $CuSO_4 \cdot 5H_2O$ solution for about 3 hours, and washed it with ultra-pure water to remove dissociate Cu. After that, the Cu-PDTPP/GC electrode was dried at room temperature for subsequent characterization.

The PDTPP/C/GC electrode was obtained by taking the C/GC electrode as the working electrode for the polymer fabrication of the PDTPP on the C/GC, and the procedure was just as that of the PDTPP/GC electrode. In like the same manner, the Cu-PDTPP/C/GC electrode was prepared by soaking the PDTPP/C/GC electrode in the $CuSO_4 \cdot 5H_2O$ solution for about 3 hours. The synthetic routes of four catalysts including Cu-PDTPP/C/GC was shown in the Scheme 1.



Scheme 1. Schematic diagram of synthetic process of Cu-PDTPP (a), and the preparation procedure of the catalysts (b) including PDTPP/GC, Cu-PDTPP/GC, PDTPP/C/GC and Cu-PDTPP/C/GC.

2.3 Physical characterization and electrochemical measurements

Scanning electron microscope (SEM, SU 8020) technique was used to recognize appearance features of samples under a 1.0 kV of accelerating voltage. The surface element composition of catalysts were recorded on Thermal Scientific X-ray photoelectron spectroscopy (ESCALAB 250Xi) under an ultrahigh vacuum ($<10^{-9}$ mbar) by using monochromatic Al K α (1486.6 eV) as radiation source.

The samples used for SEM and XPS were prepared taking ITO electrode as the conducting surface instead of GC electrode as the surface. In this case, the C/GC surface was represented by the C/ITO surface, which was prepared as follows: 30 μ L the ink dispersion was drop on the ITO coated glass, dried under room temperature. And then the C/ITO was coated with the PDTPP polymer under a constant potential of 1.3 V and the polymerization charge was of 0.05 C in a area of 0.5×0.5 cm 2 . The Cu-PDTPP/C/ITO electrode was made by immersing PDTPP/C/ITO in CuSO $_4$ solution for 3 hours, which represented the Cu-PDTPP/C/ITO electrode.

All the electrochemical measurements for these catalysts were conducted at room temperature in PBS solution (0.1 M), which was purged with high-purity O $_2$ or N $_2$ for about 30 minutes to obtain the O $_2$ - or N $_2$ -saturated electrolyte before each measurement. Cyclic voltammetry (CV), rotating disk electrode (RDE) were carried out with a conventional three-electrode. The modified GC electrode (5 mm diameter, 0.196 cm 2) was used as the working electrode, the platinum wire and Ag/AgCl/sat. KCl electrode (0.197 V+0.0591*pH vs. RHE at 25 $^{\circ}$ C) were respectively counter and reference electrode. Cyclic voltammetry was firstly cycling for 20 cycles between -0.8 and 0.5V to activate the working

electrode. Furthermore, all of these technique (CV, RDE) were tested by Autolab potentiostat/galvanostat (PGSTAT 302N) and electrode rotator (AFMSRCE, Pine) stations.

3. RESULTS AND DISCUSSION

3.1 Physical characterizations

As shown in Figure.1, the microstructure images of C/ITO, PDTPP/C/ITO and Cu-PDTPP/C/ITO were characterized by SEM measurement. The irregular spherical structure of carbon particles were shown in Figure.1a with a particle size of 50-100 nm. The carbon image demonstrated a porous feature which is greatly beneficial to the diffuse of oxygen and water, explaining the carbon can be used as an effective supporting material for ORR catalysts.

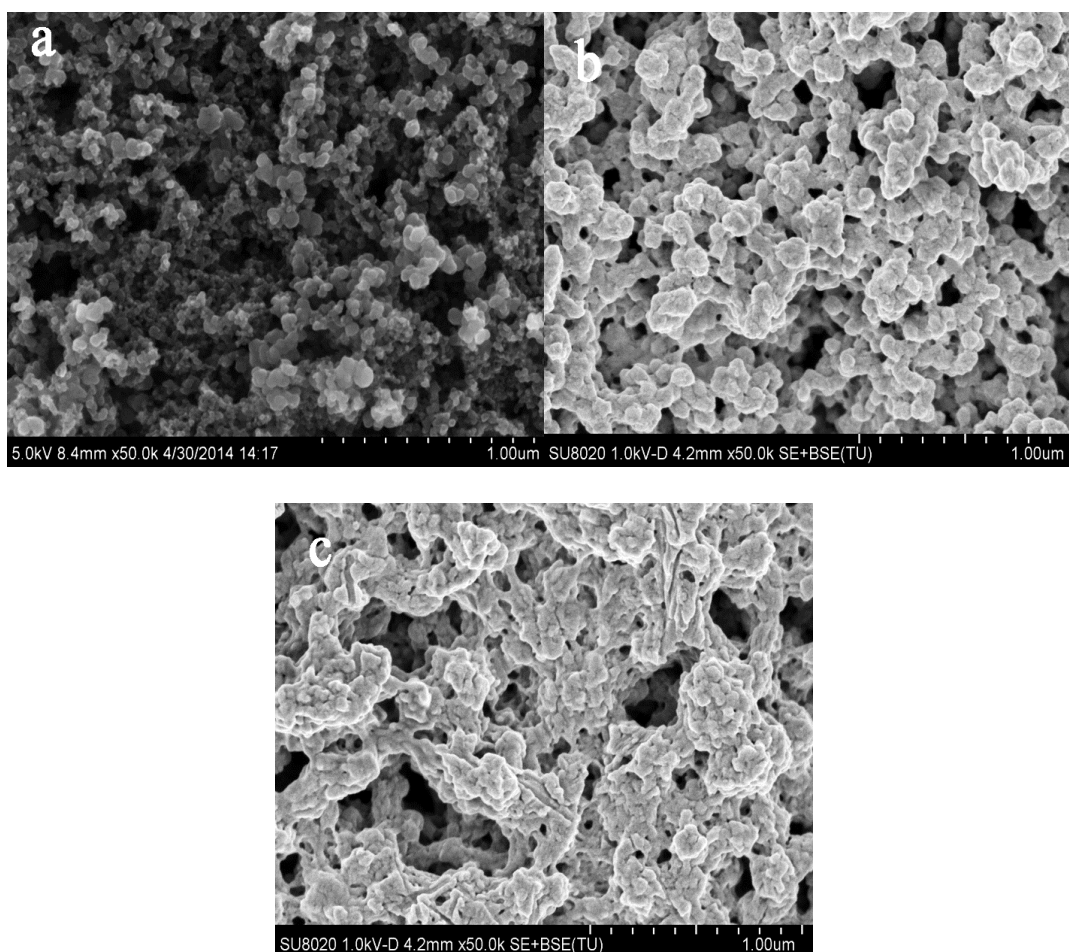


Figure. 1. Typical SEM images of (a) Vulcan XC-72/C/ITO (b) PDTPP/C/ITO (c) Cu-PDTPP/C/ITO catalysts.

Furthermore, the newly synthesized catalyst PDTPP/C/ITO has a larger particle (100-130 nm) and aperture size compare to carbon particles which can be observed in Figure.1b, the uniform rod-like

particles of PDTTP/C/ITO initially described polymers PDTTP have been successfully loaded on the surface of carbon [21-22]. After complexation with copper, the minor changes between PDTTP/C/ITO and Cu-PDTTP/C/ITO can be realized in morphology and particle size as shown in Figure.1c. The bigger particles (135-140 nm) of Cu-PDTTP/C/ITO went together to form a network structure which proved the successfully coordination of metal ion onto the polymer surface. In general, with the increasing particle size and the changing apparent structure, we can confirm the formation of new catalysts PDTTP/C/ITO, Cu-PDTTP/C and these new materials were expect to exhibit good electrochemical performances in later tests.

High-resolution XPS spectra were used to confirm the surface element containing of PDTTP/C/ITO, Cu-PDTTP/C/ITO catalysts. Figure.2 shows the N 1s spectra of PDTTP/C/ITO, Cu-PDTTP/C/ITO and the Cu 2p spectra of Cu-PDTTP/C/ITO respectively. As we can see in Figure.2a, the N 1s peaks of PDTTP/C/ITO contained two types of nitrogen species including pyridinic-type N (398.4 eV) and quarternary-type N (401.1 eV). The primary peak located at 398.4 eV can be assigned to pyridinic type nitrogen contained in the polymer due to the presence of the phenanthroline unit and the quinoxaline unit. Compared with PDTTP/C/ITO, the N 1s spectra of Cu-PDTTP/C (Figure.2b) showed the same peaks with a different position.

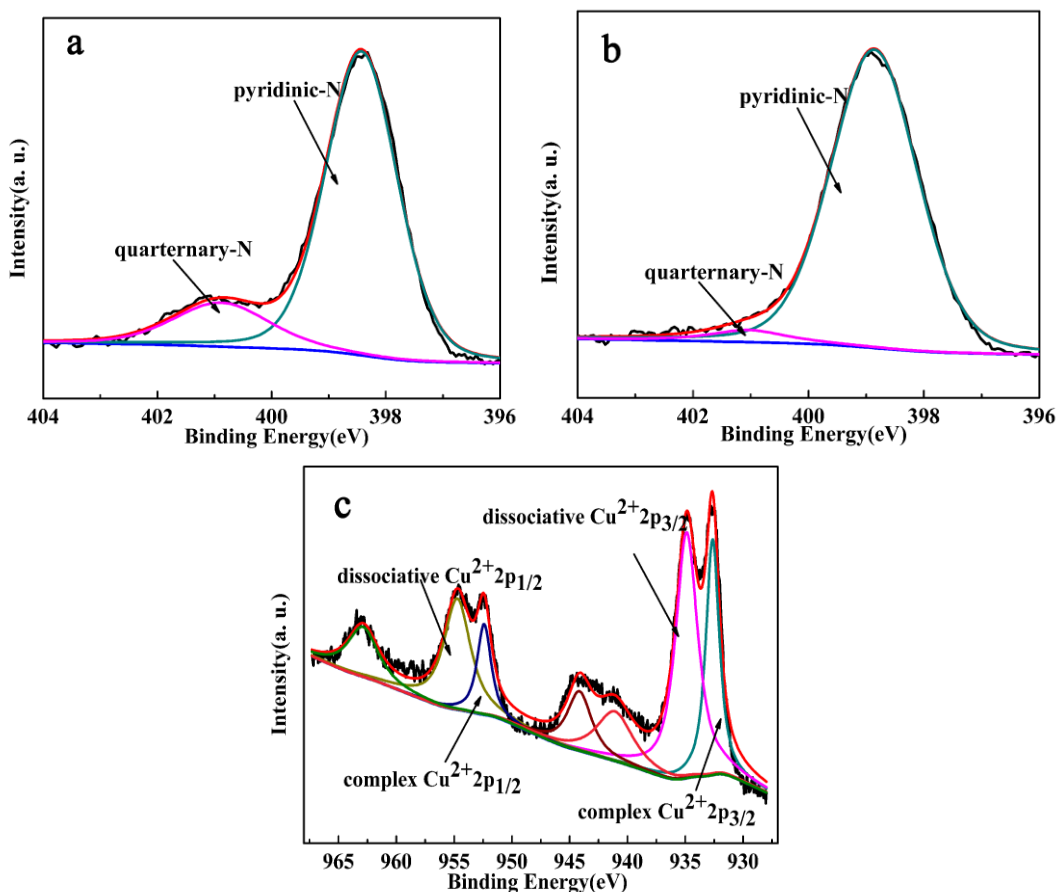


Figure. 2. XPS spectrum including N 1s peaks of PDTTP/C/GC (a), Cu-PDTTP/C/GC (b) and the Cu 2p peaks of the Cu-PDTTP/C/GC catalyst (c).

The pyridinic-type N in Cu-PDTPP/C/ITO shifted to 398.8 eV from 398.4 eV which may attribute to the successfully coordination of copper to PDTPP/C/ITO. It is worth noting that the pyridinic-type N not only play a significant part in enhancement of electrocatalytic activity but also provide a coordinating site for metal ions in the catalyst. And the functions of this type of nitrogen had been discussed in previous literature [23-25]. In addition, to further confirm the successful coordination of copper ions, Cu 2p spectra of Cu-PDTPP/C/ITO were shown in Figure.2c. Two pairs of pronounced peaks can be observed which represent the two kinds of characteristic peaks of copper. The peaks located at 934.9 eV and 954.8 eV may belong to typical dissociative Cu^{2+} $2p_{3/2}$ and Cu^{2+} $2p_{1/2}$ peaks respectively. While the Cu^{2+} $2p_{3/2}$ and Cu^{2+} $2p_{1/2}$ values of 932.7 eV and 952.5 eV, respectively, might be an indication of the formation of the complex between the copper ion and the PDTPP polymer. On this occasion, it is can be seen that the expected Cu-PDTPP/C/ITO (i.e. Cu-PDTPP/C/ITO) catalyst was produced. Furthermore, the two similar peaks situated at 940.9 eV and 944.1 eV shown in Fig.C can be assigned to CuO $2p_{3/2}$ which was formed largely due to the oxidation of dissociative copper in reaction solution. All of these results indicated that the expected catalysts including PDTPP/GC, Cu-PDTPP/GC, PDTPP/C/GC, Cu-PDTPP/C/GC could be prepared by the methods as ascribed in the former section.

3.2 CV measurements

The electrocatalytic activities of these catalysts were firstly estimated by cyclic voltammetry method. The CV curves of PDTPP/GC, PDTPP/C/GC, Cu-PDTPP/GC, Cu-PDTPP/C/GC measured in N_2 -saturated and O_2 -saturated 0.1 M PBS buffer aqueous solution were respectively shown in Figure.3. Cyclic voltammetry curves of different catalysts showed different shapes with an obvious deoxidization peak and it can be found that significant changes have taken place on each pair of CV curves. The maximum peak current density exhibited an obvious enhancement in O_2 -saturated solution compared with the peak current measured under a N_2 -saturated condition, indicating all of the four catalysts possess the ORR activity. The values of maximum peak current density displayed a clear trend that Cu-PDTPP/C/GC (-0.3047 mA) > Cu-PDTPP/GC (-0.258 mA) > PDTPP/C/GC (-0.1481 mA) > PDTPP/GC (-0.09445 mA). In addition, the ORR peak potential of Cu-PDTPP/C/GC located at 0.3893 V vs. RHE, as seen in Figure.3, which shifts more positive than that of Cu-PDTPP/GC (0.2745 V), PDTPP/C/GC (0.1329 V) and PDTPP/GC (-0.0306 V). These results proved that Cu-PDTPP/C/GC catalyst has the best ORR activity with the highest peak current density and the most positive initial oxygen reduction potential, and also confirmed the positive effects of carbon supporter and metal ions on the ORR activities on the catalysts.

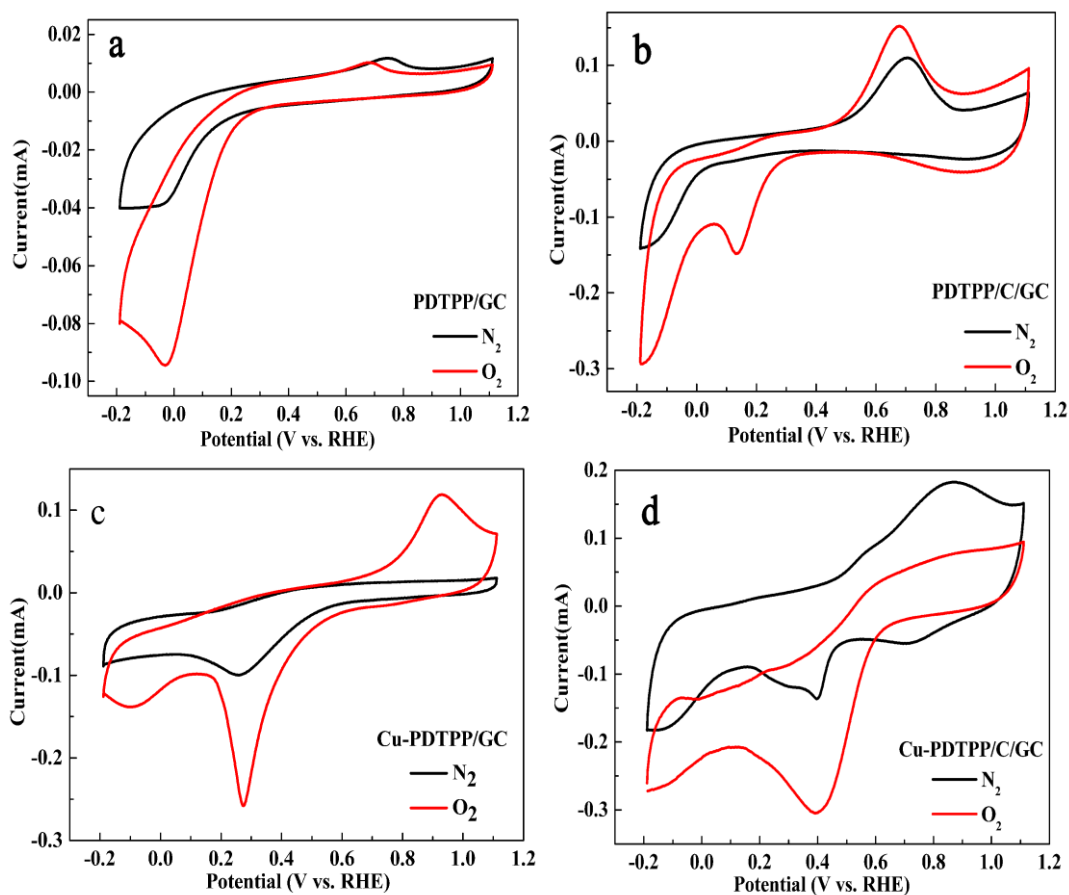


Figure 3. (a), (b), (c), (d) CV curves of PDTTP/GC, PDTTP/C/GC, Cu-PDTTP/GC, Cu-PDTTP/C/GC measured in O_2 -saturated and N_2 -saturated 0.1 M PBS (pH=7) aqueous solution range from -0.2 to 1.1 V vs. RHE. Scan rate is of 100 mV s^{-1} .

Meanwhile, the electrochemical stability is an important parameter to characterize the catalytic performance of the catalysts for ORR. The CV curves of PDTTP/GC, PDTTP/C/GC, Cu-PDTTP/GC, Cu-PDTTP/C/GC were conducted between -0.2 and 1.1 V vs. RHE in O_2 -saturated 0.1 M PBS solution for 500 cycles with a scan rate of 100 mV s^{-1} . After scanning 500 curves, a slight decline can be noticed in maximum current density of these catalysts, as shown in Figure 4. Through simple calculation, the reduction in peak currents (oxygen reduction) were 9.75%, 8.24%, 14.8% and 8.01%, respectively, for PDTTP/GC, PDTTP/C/GC, Cu-PDTTP/GC, Cu-PDTTP/C/GC. Apparently, Cu-PDTTP/C/GC illustrated the minimal loss and the best electrochemical stability among the four catalysts. From the comparison, we can also found that the catalyst loaded with carbon materials showed a less decay than other catalysts, indicated that the presence of carbon supporters could improve the stability of the catalyst in electrochemical tests.

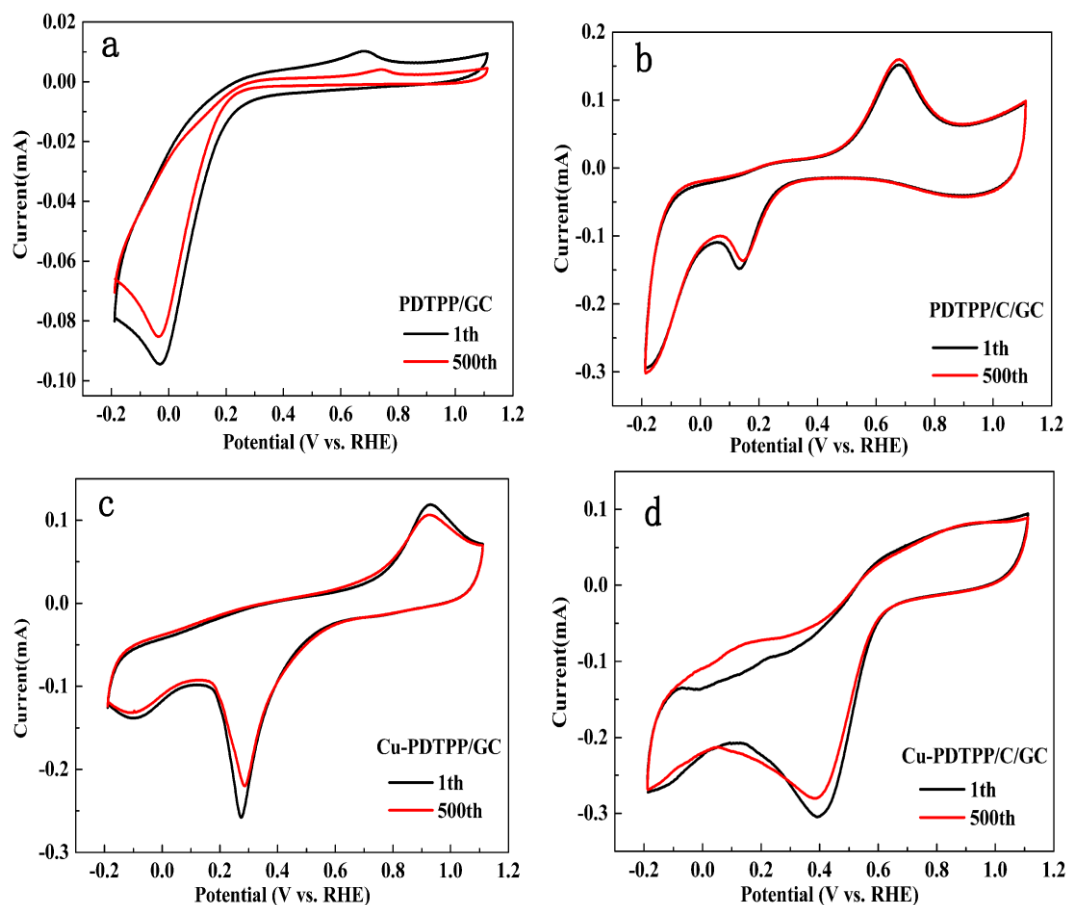


Figure 4. (a), (b), (c), (d) CV curves of PDTTP/GC, PDTTP/C/GC, Cu-PDTTP/GC, Cu-PDTTP/C/GC measured in O_2 -saturated 0.1 M PBS (pH=7) aqueous solution for 500 cycles between -0.2 and 1.1 V vs. RHE. Scan rate, 100 mV s^{-1} .

3.3 RDE measurements

To further compare the electrochemical behaviors, rotating disk electrode (RDE) method was also used to test polarization curves of four catalysts (Figure.5). The linear scanning voltammetry curves were measured in O_2 -saturated 0.1 M PBS solution with a scan rate of 10 mV s^{-1} . And, the rotation rates of the RDE electrode were fixed in the range of 400 rpm, 625 rpm, 900 rpm, 1225 rpm and 1600 rpm. Similarly, as shown in Figure.5, the obvious differences between the shapes of the catalysts can be noticed in the LSV curves of the catalysts. In addition to the differences in shapes, it also can be observed that the onset reduction potential of each catalyst kept a constant value in different rotation rates, and the current densities exhibited a uniform increase with the continuous increase in the rotation speed. The increasing current in polarization curves might due to the raising amount of oxygen participated in the catalytic process on the catalyst modified electrodes.

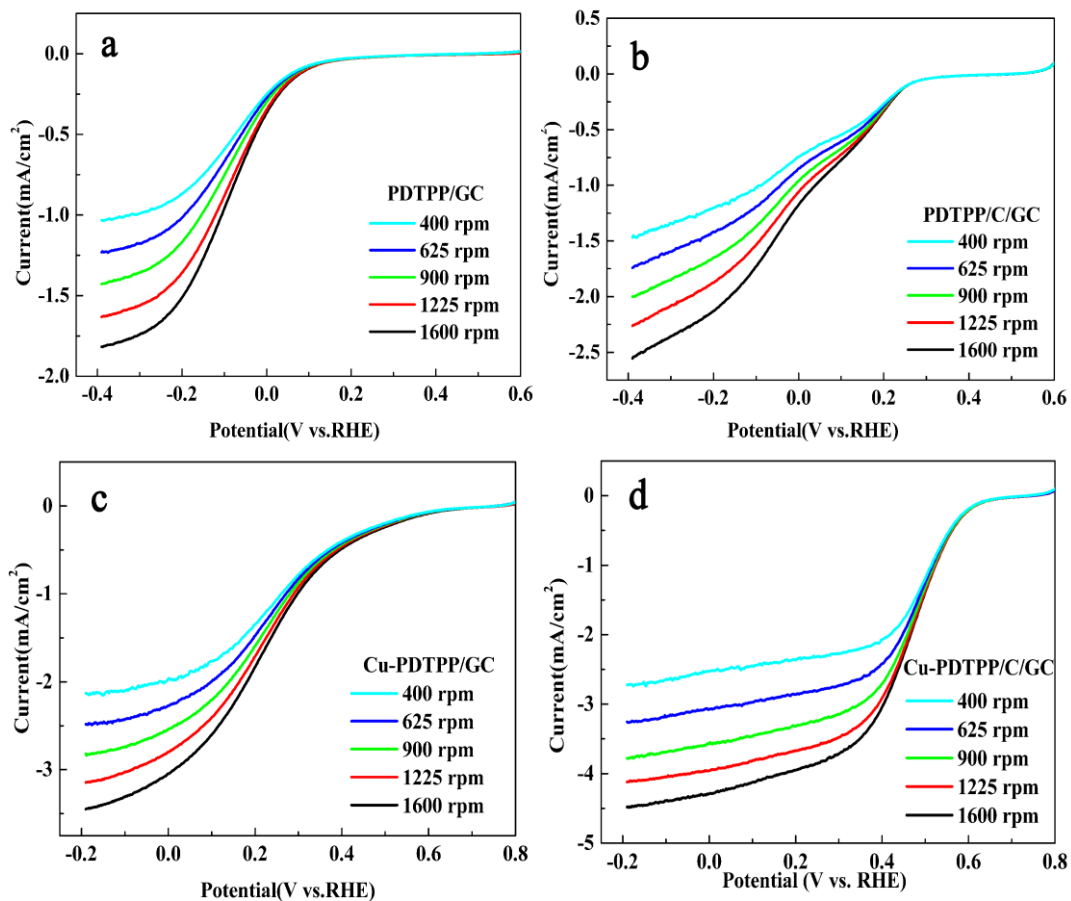


Figure 5. Linear sweep voltammograms curves of PDTPPP/GC(a), PDTPPP/C/GC(b), Cu-PDTPPP/GC(c), Cu-PDTPPP/C/GC (d) measured in O₂-saturated 0.1 M PBS with various rotation rates of 400 rpm, 625 rpm, 900 rpm, 1225 rpm, 1600 rpm. Scan rate, 10 mV s⁻¹.

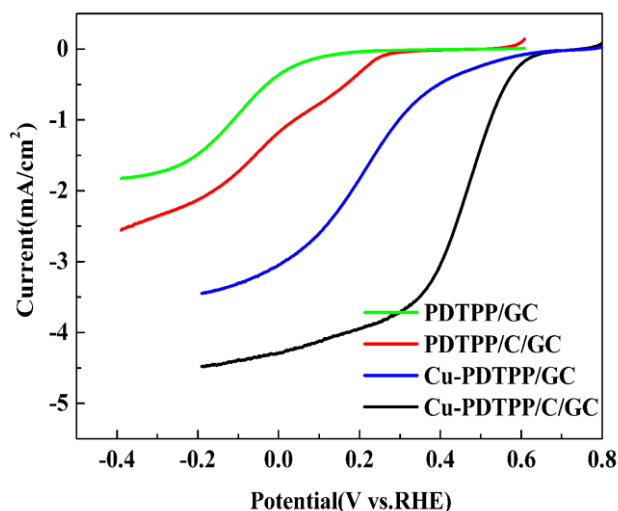


Figure 6. Polarization curves of PDTPPP/GC, PDTPPP/C/GC, Cu-PDTPPP/GC, Cu-PDTPPP/C/GC for ORR in O₂-saturated 0.1 M PBS (pH=7) aqueous solution. The potential scan rate was 10 mV s⁻¹ and the rotation speed was 1600 rpm.

In addition, in order to calculate the related parameters of the polarization curves precisely, the LSV curves of the catalysts including PDTTP/GC, PDTTP/C/GC, Cu-PDTTP/GC, Cu-PDTTP/C/GC measured at the rotation rate of 1600 rpm had been listed in Fig.6. Great disparities could be observed on the onset reduction potentials and the diffusion-limiting currents of the catalysts, which suggested their different ORR activities as well as ORR mechanisms. The onset potentials of the PDTTP/GC, PDTTP/C/GC, Cu-PDTTP/GC, Cu-PDTTP/C/GC catalyst were located at 0.1308 V, 0.2629 V, 0.6 V and 0.6412 V vs. RHE, respectively, while the diffusion-limiting currents for them are -1.82653 mA/cm^2 , -2.5551 mA/cm^2 , -3.44898 mA/cm^2 and -4.48112 mA/cm^2 , respectively. Apparently, the Cu-PDTTP/C/GC catalyst displayed the best ORR activity, which is consistent with CV results reported in the previous section.

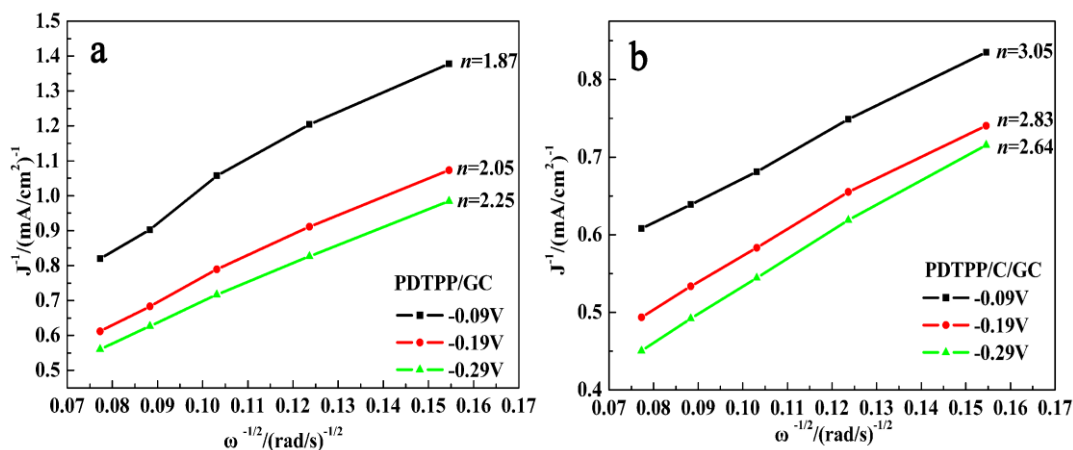
The electron transfer number of four catalysts were calculated to confirm the catalytic mechanism during oxygen reduction reaction by Koutecky-Levich (K-L) plots:[26]

$$1/J = 1/J_k + 1/J_{\text{diff}} = 1/J_k + 1/B\omega^{1/2} \quad (1)$$

$$B = 0.62nFC_0D^{2/3}\nu^{-1/6} \quad (2)$$

where J_k is the kinetic current density and J_{diff} is the diffusion-limiting current density, B is the Levich constant, ω is the angular velocity of the disk, n is the electron transfer number during the ORR, F is the Faraday constant ($F=96485 \text{ C mol}^{-1}$), C_0 is the O_2 concentration in the solution ($C_{\text{O}_2}=1.2\times 10^{-3} \text{ mol L}^{-1}$ in PH=7 0.1 M PBS solution), D is the diffusion coefficient of dissolved O_2 in the solution ($D=1.9\times 10^{-5} \text{ cm}^2 \text{ s}^{-1}$ in PH=7 0.1 M PBS solution), and ν is the viscosity of the electrolyte ($1.00\times 10^{-2} \text{ cm}^2 \text{ s}^{-1}$) [27].

It can be concluded from Figure.7, the K-L plots of catalysts all showed a good linear relationship between J^{-1} and $\omega^{-1/2}$ at different applied potentials. The electron transfer number of PDTTP/GC, PDTTP/C/GC were obtained under -0.09 , -0.19 , -0.29 V vs. RHE, while the Cu-PDTTP/GC, Cu-PDTTP/C/GC were measured under 0.21 , 0.11 , 0.01 V vs. RHE. Obviously, compared with the first two kinds of catalysts, the latter two kinds of catalysts had more positive onset reduction potentials. In such way, the potentials selected in the calculation of the electron numbers are different. According to diversities in K-L slope, four kinds of catalysts exhibit different electrons and catalytic mechanism, as shown in Fig.7.



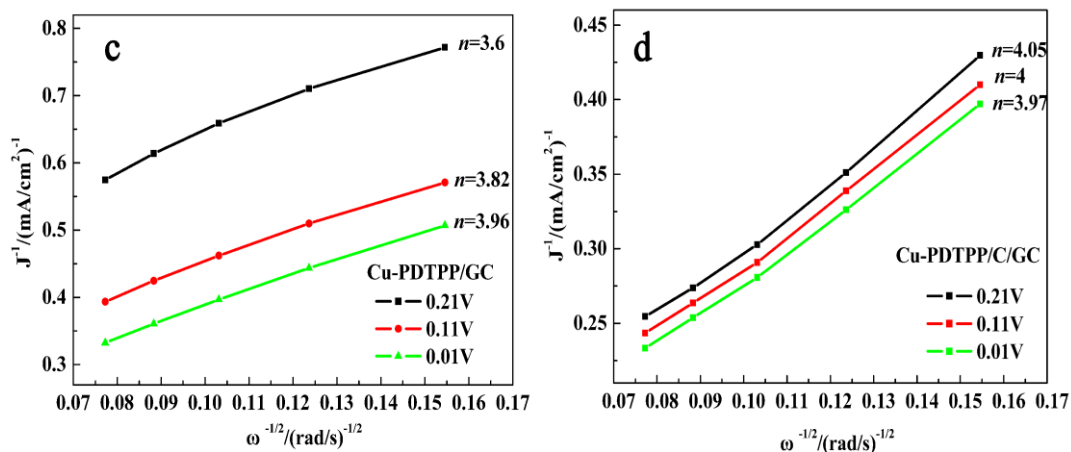


Figure 7. K-L plots and electron transfer numbers of PDTPPP/GC (a), PDTPPP/C/GC (b) at -0.09, -0.19, -0.29 V. vs. RHE and Cu-PDTPPP/GC (c), Cu-PDTPPP/C/GC (d) at 0.21, 0.11, 0.01 V. vs. RHE.

The average electron transferred numbers for PDTPPP/GC, PDTPPP/C/GC, Cu-PDTPPP/GC, Cu-PDTPPP/C/GC were calculated to be 2, 2.8, 3.8 and 4 respectively (Figure.8), indicating Cu-PDTPPP/C/GC occurred a direct 4e reduction pathway of O_2 is reduced to H_2O . While PDTPPP/C/GC and Cu-PDTPPP/GC takes a coexisting pathway involving both the 2e and 4e transfers, and PDTPPP/GC catalyst employs a two-electron reduction pathway. In this sense, Cu-PDTPPP/C/GC catalyst was a best choice not only in terms of electron transfer number and the initial reduction potentials. Table 1 showed electrochemical data had been tested for different electrodes by CV and RDE measurements.

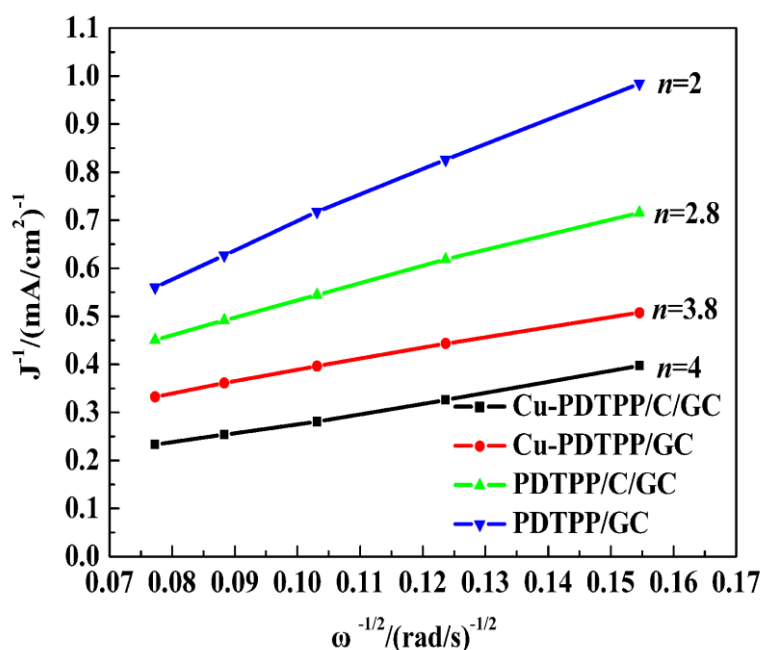


Figure 8. The yield of average electron transfer number of PDTPPP/GC, PDTPPP/C/GC, Cu-PDTPPP/GC, Cu-PDTPPP/C/GC calculated from RDE curves.

Some polymer based non noble metal ORR catalysts were also reported in recent years, and they were also not subjected to thermal treatment, and the parameters of these catalysts are summarized in Table 2. From Table 2, it is obviously found that the catalysts reported in this study especially Cu-PDTPP/C/GC have superior or equivalent catalytic activities to that of the ORR catalysts presented in Table 2[28-32].

Table 1. Comparison of the electrochemical data for different electrodes.

Modifier	E_{peak} (V vs. RHE)	I_{max} (mA)	E_{onset} (V vs. RHE)	I_{limiting} (mA/cm ²) (1600 rpm)	Average n (K-L)
PDTPP/GC	-0.0306	-0.09445	0.1308	-1.82653	2
PDTPP/C/GC	0.1329	-0.1481	0.2629	-2.5551	2.8
Cu-PDTPP/GC	0.2745	-0.258	0.6	-3.44898	3.8
Cu-PDTPP/C/GC	0.3893	-0.3047	0.6412	-4.48112	4

Table 2. The parameters related with the polymer based ORR catalyst without noble metals

Catalyst	E_{peak} (V)	E_{onset} (V)	$E_{1/2}$ (V)	n	Electrolyte solution	Reference electrode	Reference
PHTPP	0.15	0.26	0.12	2.2	PBS (pH=7.0)	RHE	28
PHTPP-Cu	0.30	0.58	0.30	3.8	PBS (pH=7.0)	RHE	28
Pt/C (20 %)	0.65	0.90	0.63	4.0	PBS (pH=7.0)	RHE	28
CuPPyPhen/C	0.37	0.62	-	4.0	PBS (pH=7.0)	RHE	29
CuINPD/C	-0.38	-0.15	-	3.1	0.1 M KNO ₃	Ag/AgCl	30
POT-Co-OMC	-0.27	-0.3	-	3.8	0.1 M KOH	Ag/AgCl	31
Poly(APT-GO)	-0.38	-0.03	-	3.5	0.1 M NaOH	Ag/AgCl	32
Poly(APT-RGO)	-	-0.06	-	2	0.1 M NaOH	Ag/AgCl	32

4. CONCLUSIONS

Four non noble metal catalysts for oxygen reduction were prepared based on conductive polymers, carbon black and copper ion (II). The catalysts could be fancily deposited on the glassy carbon electrode and the procedure was very simple and continent. The nitrogen-riched polymer could be electropolymerized on the electrode with a low potential, which contained the phenanthroline unit for metal ion complexation. The electrochemical activities of these catalysts were measured by CV and RDE method, while the compositions of the catalysts were confirmed with SEM and XPS methods. The CV curves of different catalysts demonstrated the catalysts with carbon supporters showed superior stabilities than the carbon absent catalysts. It was also observed in LSV curves that the Cu-PDTPP/C/GC catalyst showed a excellent current density and onset potential than other catalyst, which suggested the M-N_x unit in the catalyst composites played a key role for ORR activity. The Cu-PDTPP/C/GC catalyst has a potential application as cathode catalyst in fuel cells, such as microbial fuel cell, which performed in a neutral aqueous medium.

ACKNOWLEDGEMENTS

The work was financially supported by the National Natural Science Foundation of China (31400044).

References

1. M. I. Qureshi, A. M. Rasli, K. Zaman, *J Clean Prod.*, 112 (2016) 3657.
2. G. Zsurka, W. S. Kunz, *Lancet Neurol.*, 14 (2015) 956.
3. L. Carrette, K. Friedrich, U. Stimming, Fuel cells, 1 (2001) 5.
4. X. S. Hu, N. Murgovski, L. M. Johannesson, B. Egardt, Mechatronics, *IEEE/ASME Trans. Mechatronics.*, 20 (2015) 457.
5. H. Huang, J. Lin, Y. L. Wang, S. R. Wang, C. R. Xia, C. H. Chen, *J. Power Sources.*, 274 (2015) 1114.
6. S. Vierrath, F. Güder, A. Menzel, M. Hagner, R. Zengerle, M. Zacharias, S. Thiele, *J. Power Sources.*, 285 (2015) 413.
7. T. Nagai, S. Yamazaki, N. Fujiwara, M. Asahi, Z. Siroma, T. Ioroi, *J. Electrochem. Soc.*, 163 (2016) F347.
8. M. Kannan, *Biosens. Bioelectron.*, 77 (2016) 1208.
9. V. R. Stamenkovic, B. Fowler, B. S. Mun, G. F. Wang, P. N. Ross, C. A. Lucas, N. M. Marković, *Sci.*, 315 (2007) 493.
10. V. R. Stamenkovic, B. S. Mun, M. Arenz, K. Mayrhofer, C. A. Lucas, G. F. Wang, P. N. Ross, N. M. Markovic, *Nat. Mater.*, 6 (2007) 241.
11. V. Stamenkovic, B. S. Mun, K. Mayrhofer, P. N. Ross, N. M. Markovic, J. Rossmeisl, J. Greeley, J. K. Nørskov, *Angew. Chem. Int. Ed.*, 118 (2006) 2963.
12. U. A. Paulus, A. Wokaun, G. G. Scherer, T. J. Schmidt, V. Stamenkovic, V. Radmilovic, N. M. Markovic, P. N. Ross, *J. Phys. Chem. B*, 106 (2002) 4181.
13. J. Suntivich, H. A. Gasteiger, N. Yabuuchi, H. Nakanishi, J. B. Goodenough, Y. Shao-Horn, *Nat Chem.*, 3 (2011) 546.
14. H. J. Lee, J. H. Lee, S. Y. Chung, J. W. Choi, *Angew. Chem. Int. Ed.*, 128 (2016) 1521.
15. A.S. Ryabova, F. S. Napol'skiy, T. Poux, S. Y. Istomin, A. Bonnefont, D. M. Antipin, A. Y. Baranchikov, E. E. Levin, A. M. Abakumov, G. Kéranguéven, *Electrochim. Acta*, 187 (2016) 161.
16. A. Zhao, J. Masa, M. Muhler, W. Schuhmann, W. Xia, *Electrochim. Acta*, 98 (2013) 139.
17. Z. Y. Liu, G. X. Zhang, Z. Y. Lu, X. Y. Jin, Z. Chang, X. M. Sun, *Nano Res.*, 6 (2013) 293.
18. H. J. Tang, H. J. Yin, J. Y. Wang, N. L. Yang, D. Wang, Z. Y. Tang, *Angew. Chem.*, 125 (2013) 5695.
19. S. S. Zhu, T. M. Swager, *J. Am. Chem. Soc.*, 119 (1997) 12568.
20. Y. Tsubata, T. Suzuki, T. Miyashi, Y. Yamashita, *J. Org. Chem.*, 57 (1992) 6749.
21. G. R. Chalmers, R. M. Bustin, I. M. Power, *AAPG Bull.*, 96 (2012) 1099.
22. J. Cravillon, C. A. Schröder, H. Bux, A. Rothkirch, J. Caro, M. Wiebcke, *CrystEngComm.*, 14 (2012) 492.
23. S. Malmgren, K. Ciosek, M. Hahlin, T. Gustafsson, M. Gorgoi, H. Rensmo, K. Edström, *Electrochim. Acta*, 97 (2013) 23.
24. K. Mudiyansele, S. D. Senanayake, L. Faria, S. Kundu, A. E. Baber, J. Graciani, A. B. Vidal, S. Agnoli, J. Evans, R. Chang, *Angew. Chem. Int. Ed.*, 52 (2013) 5101.
25. B. Philippe, R. Dedryvère, J. Allouche, F. Lindgren, M. Gorgoi, H. Rensmo, D. Gonbeau, *Chem. Mater.*, 24 (2012) 1107.
26. W. Y. Wong, W. R. W. Daud, A. B. Mohamad, K. S. Loh, *Int. J. Hydrogen Energy*, 40 (2015) 11444.
27. Y. Gochi-Ponce, G. Alonso-Nuñez, N. Alonso-Vante, *Electrochem. Commun.*, 8 (2006) 1487.
28. H. Y. He, M. Wang, J. S. Zhao, Y. Zhang, *Chem. Eng. J.*, 316 (2017) 680.

29. Y. Lu, X. Wang, M. Wang, L. Kong, J. Zhao, *Electrochim. Acta*, 180 (2015) 86.
30. J. Yu, Y. Lu, C. Yuan, J. Zhao, M. Wang, R. Liu, *Electrochim. Acta*, 143 (2014) 1.
31. J. Ju, X. Bo, H. Wang, Y. Zhang, C. Luhana, L. Guo, *Electrochem. Commun.*, 25 (2012) 35.
32. M. H. Naveen, H. B. Noh, M. S. Al Hossain, J. H. Kim, Y. B. Shim, *J. Mater. Chem. A*, 3 (2015) 5426.

© 2017 The Authors. Published by ESG (www.electrochemsci.org). This article is an open access article distributed under the terms and conditions of the Creative Commons Attribution license (<http://creativecommons.org/licenses/by/4.0/>).